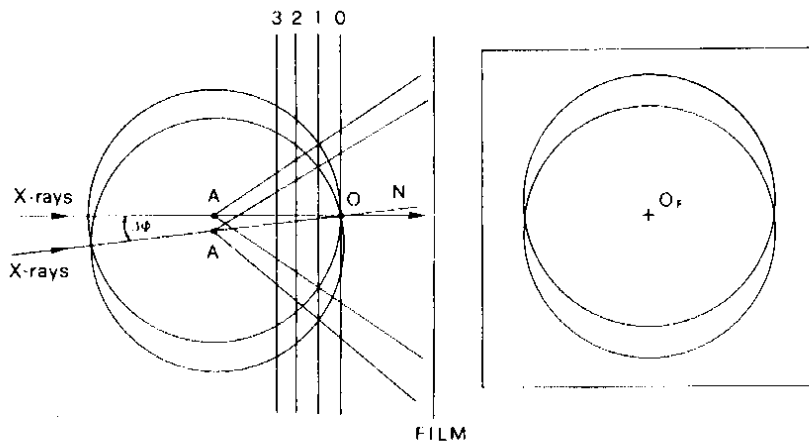


### Geometry of the rotation method

In the rotation method a crystal is made to rotate or oscillate, that is it is moved back and forth, through a small angle about one axis perpendicular to the X-ray beam and the diffracted intensities are recorded on a flat film (that can also be V-shaped) contained in a cassette perpendicular to the incident X-rays (see Fig. 4.27). Small rotation angles are required to avoid reflection overlap on the film. An asymmetric unit of reciprocal space is covered by successively exposing different cassettes.

When we discussed the Weissenberg camera, we saw that reciprocal lattice planes perpendicular to the rotation axis generate a series of layer lines on a cylindrical film. Let us now see what happens if we have a flat film perpendicular to the X-ray beam as shown in Fig. 4.27. In describing a crystal rotation, it is easier, and therefore often preferred, to leave the reciprocal lattice fixed and move instead the Ewald sphere. When the crystal is rotated a small angle  $\Delta\Phi$ , the two circles that result from the intersection of the Ewald sphere at the beginning and end of the rotation range and each reciprocal lattice plane, define two crescent-shaped lunes



**Fig. 4.27.** The rotation motion. The motion is shown leaving the reciprocal lattice planes fixed and rotating the Ewald sphere about the point O. After the spindle has rotated an angle  $\Delta\Phi$ , the intersections of the Ewald sphere with each reciprocal lattice plane define two lunes per plane. A pair of lunes is shown on the right-hand side. The film is placed flat and normal to the X-ray beam. During the rotation of the crystal it is kept stationary.

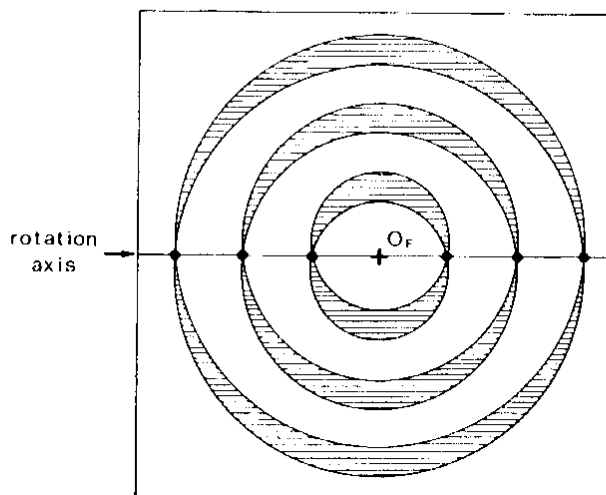


Fig. 4.28. Projection of the intersections of the Ewald sphere and three reciprocal lattice planes on the film. The innermost pair of lunes corresponds to the plane with index one because the plane with index zero is tangential to the Ewald sphere.

that contain all the reciprocal lattice points that will produce diffraction on the flat film perpendicular to the X-ray beam. Thus a rotation photograph contains reflections coming from all the reciprocal layers that intersect the Ewald sphere as shown in Fig. 4.28. The reflections contained in each of the lunc pairs come from the same reciprocal lattice plane and therefore have one index in common.

Since nodes in reciprocal space have a volume, a reflection is not completely recorded on the film until the entire volume has passed through the Ewald sphere. Any reflection whose reciprocal lattice node has not completely passed through the Ewald sphere is called a partially recorded reflection or, more improperly, half spot, regardless of the percentage of the volume that has passed through the sphere of reflection. Since the rotation range in macromolecular crystallography is usually quite small, as we will see, a substantial number of reflections on a rotation film are partially recorded reflections. These have to be properly identified and dealt with during film processing. One of the reasons why the rotation method has been so successful is that it has been found that reflections partially recorded on different films can be added together<sup>[38]</sup> to yield a reliable value for the total diffracted intensity.

Figure 4.29 shows the idealized shape of the partially recorded reflections, which is different if they are recorded at the beginning or the end of the rotation range. In one case the missing part of the reflection has been recorded in the previous film, in the other it will be recorded on the next. Re-examining Fig. 4.28 we notice that the area of reciprocal space that crosses the Ewald sphere becomes a series of points along the projection of the rotation axis. Thus, no matter how small their reflecting range, reflections found along this line will always be partially recorded.

Wonacott<sup>[39]</sup> has examined the factors that limit the maximum rotation range allowed without having reflection overlap from different reciprocal lattice planes on the film. The expression for the maximum rotation range is:

$$\Delta\Phi_{\max} \leq |r^*|/R_{\max}^* - \Delta \tag{4.29}$$

where  $\Delta\Phi_{\max}$  is the maximum allowed rotation range in radians,  $R_{\max}^*$  the

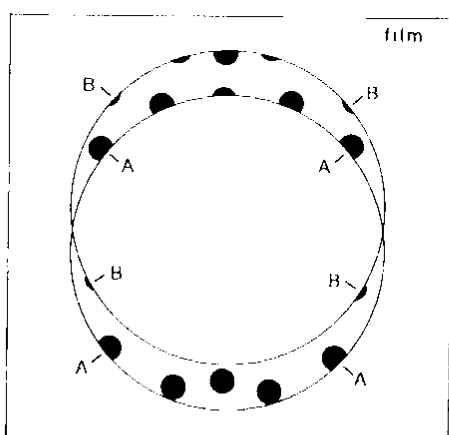


Fig. 4.29. The idealized shape of partially recorded reflections. The spots labelled A are recorded at one end of the rotation range and those labelled B at the other end. The missing parts of reflections A will be found on the previous rotation photograph and those of spots B on the following one.

maximum resolution in reciprocal space of the data that will be collected,  $r^*$  is the pertinent reciprocal lattice vector, and  $\Delta$  is the reflecting range of the crystal.

As an example let us calculate  $\Delta\Phi_{\max}$  for a maximum resolution of 2.5 Å when the relevant reciprocal lattice vector is 1/100 Å and  $\Delta$  is 0.4°

$$\Delta\Phi_{\max} \approx 2.5/100 \times 57.3 - 0.4 = 1^\circ$$

where we have multiplied by 57.3 to convert radians into degrees.

In Fig. 4.30 the Ewald sphere is represented projected onto the plane determined by the X-ray beam and the crystal rotation axis. A limiting sphere of smaller radius represents the maximum resolution of the data that will be collected in the rotation experiment. The maximum rotation range of the crystal, represented by a 360° rotation of the Ewald sphere about the rotation axis, will cover the volume of reciprocal space limited by the toroid generated by the rotation of the sphere but will leave out the shaded volume shown projected onto the plane of the figure, a blind zone inaccessible to the rotation geometry. From the figure it should be apparent that the volume of the blind region increases with the resolution of the data to be collected. A plot of the percentage of reciprocal space which cannot be measured in a rotation experiment as a function of the resolution desired has been calculated by Wonacott.<sup>1391</sup> For data of up to 5 Å resolution, it is only 0.72 per cent but it increases to 4.58 per cent for 2.0 Å resolution. In order to record the data generated by the reciprocal lattice nodes present in the blind region, the crystal has to be rotated about a different axis.

Figure 4.31 shows the total volume of reciprocal space swept out as the crystal is rotated a total angle of 30°, 90°, and 180°. From the figure it should be evident that even if the rotation axis has no symmetry it is never necessary to rotate a crystal much more than 180° in order to collect all of reciprocal space with the exception of the blind region, not represented in the figure. The volume which has not been covered by a 180° rotation has been dotted in Fig. 4.31(c) and its size depends on the resolution desired as shown in the same figure. From the figure it should also be clear that, in

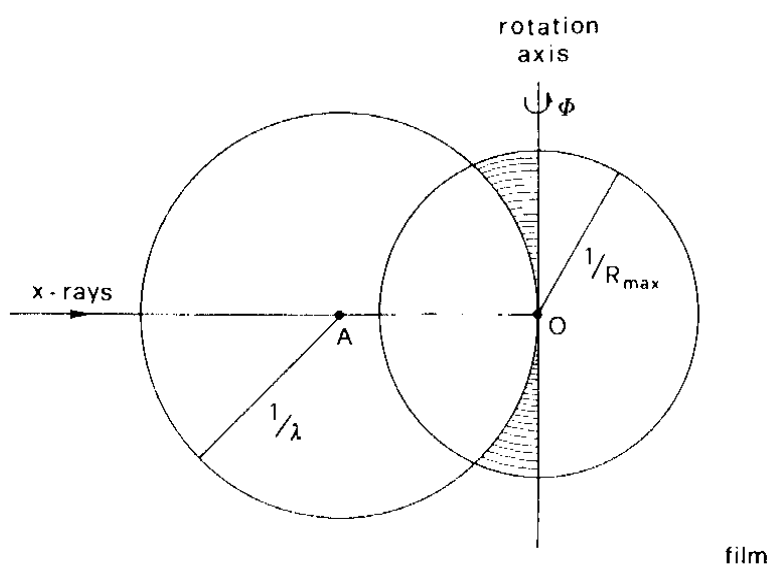
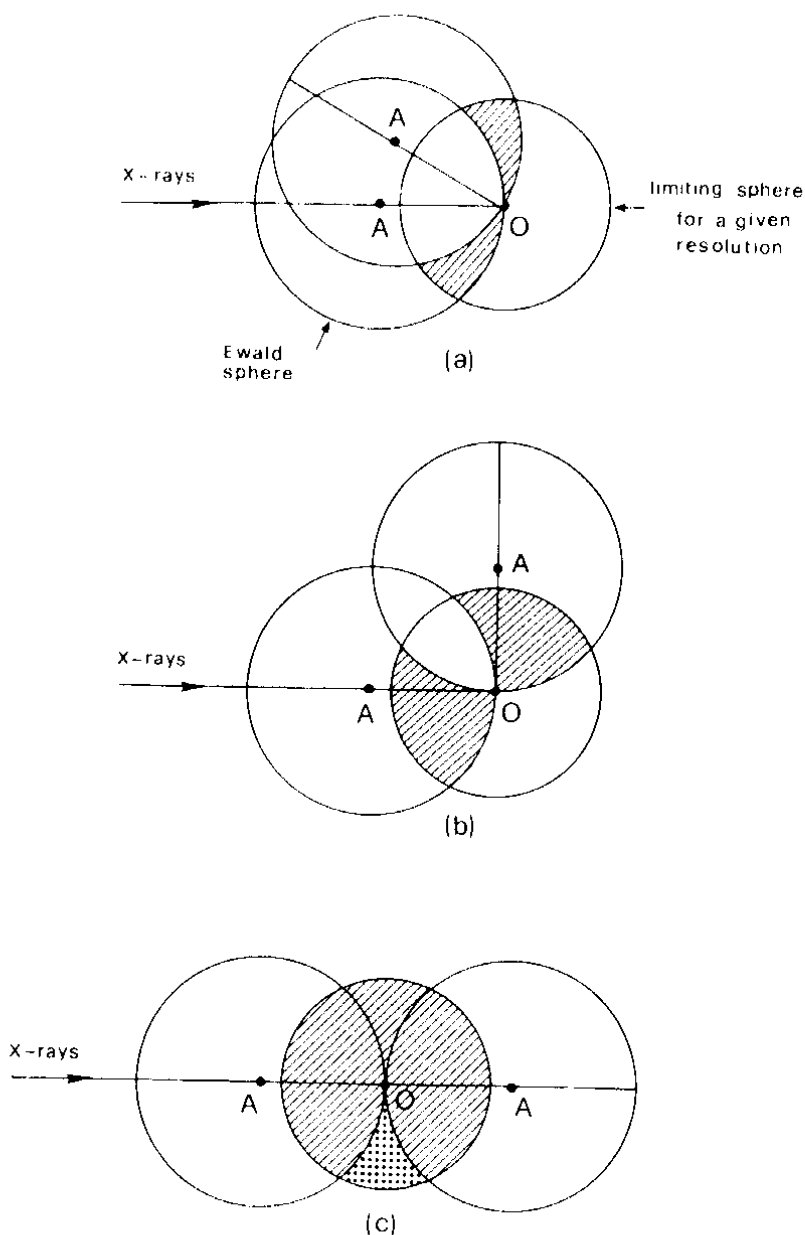


Fig. 4.30. Rotation geometry showing the Ewald sphere projected on to the plane defined by the X-ray beam and the rotation axis. A limiting sphere centred on O shows the resolution desired or attainable. The shaded region represents the volume of reciprocal space inaccessible to the rotation movement.



**Fig. 4.31.** Volume of reciprocal space explored by a total rotation range of 30° (a), 90° (b), and 180° (c). In each case a limiting sphere corresponding to a chosen resolution defines the volume of reciprocal space of interest.

order to minimize the total rotation range, it is desirable to rotate the crystal about the crystallographic axis of highest symmetry. Thus if a hexagonal crystal is rotated about the  $c$  axis, a 30° total rotation range will suffice to cover a reciprocal space asymmetric unit in which the only missing volume will be the blind region.

Symmetry is, however, not the only consideration in the choice of the rotation axis. Another factor, which is equally important, is the size of the unit cell parameters. We have seen that the maximum rotation interval per photograph is dependent on the unit cell parameters. Ideally, one would like to rotate about the axis with the largest unit cell parameter, which in this way does not become a limiting factor in the choice of the maximum

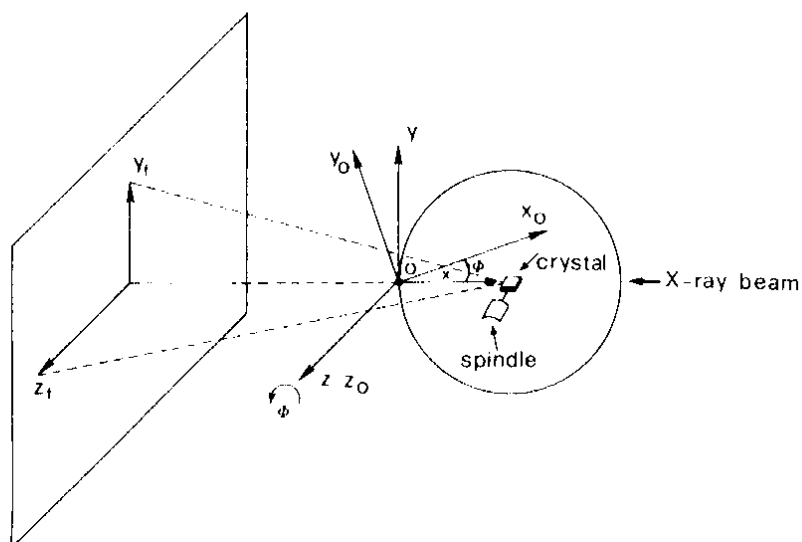


Fig. 4.32. The crystal, laboratory, and film coordinate systems. The origin of crystal and laboratory systems is at the intersection of the X-ray beam with the Ewald sphere. The origin of the film system at the intersection of the X-ray beam with the film.

rotation range per photograph. Still, there may be practical reasons that partially or totally limit the freedom of choice of the rotation axis. An example is crystal morphology. A crystal shaped as a very thin plate with its highest symmetry axis perpendicular to the plate cannot be easily mounted with that axis parallel to the spindle.

### Calculation of the film coordinates for a reflection

In order to calculate the film coordinates for a reflection, four different sets of coordinate systems have to be introduced. The first is the crystallographic reciprocal lattice with its unit vectors  $\mathbf{a}^*$ ,  $\mathbf{b}^*$ , and  $\mathbf{c}^*$  and the angles  $\alpha^*$ ,  $\beta^*$ , and  $\gamma^*$ . In this coordinate system, a reciprocal lattice point is specified by the vector  $\mathbf{r}^*$  (see p. 65).

$$\mathbf{r}^* = h\mathbf{a}^* + k\mathbf{b}^* + l\mathbf{c}^*.$$

The second coordinate system is an orthogonal system called the crystal coordinate system which is linked to the crystal, that is it rotates just as  $\mathbf{a}^*$ ,  $\mathbf{b}^*$ , and  $\mathbf{c}^*$  and differs from it in that it is always orthogonal (see Fig. 4.32).

In this new coordinate system, the coordinates of a reciprocal lattice point,  $(x_0, y_0, z_0)$  can be calculated as follows

$$\begin{aligned} x_0 &= ha_x^* + kb_x^* + lc_x^* \\ y_0 &= ha_y^* + kb_y^* + lc_y^* \\ z_0 &= ha_z^* + kb_z^* + lc_z^* \end{aligned} \quad (4.30)$$

where  $a_x^*$  is the projection of  $\mathbf{a}^*$  onto the  $x_0$  axis, etc.

The third coordinate system is the laboratory orthogonal coordinate system which remains fixed as the crystal is rotated. This system is defined so that  $z$  is parallel to the rotation axis and  $x$  is parallel to the X-ray beam but points in the opposite direction. If at the beginning of the rotation experiment the crystal and laboratory coordinate systems coincide, after the crystal has rotated a certain angle  $\Phi$ , the coordinates of a point in the

laboratory system will be

$$\begin{aligned} x &= x_0 \cos \Phi + y_0 \sin \Phi \\ y &= y_0 \cos \Phi - x_0 \sin \Phi \\ z &= z_0 \end{aligned} \tag{4.31}$$

as can be seen in Fig. 4.32. If the angle  $\Phi$  at which a given reciprocal lattice point crosses the Ewald sphere is known, since  $x_0$ ,  $y_0$ , and  $z_0$  are only functions of the reflection indices and the unit cell parameters,  $x$ ,  $y$ , and  $z$ , the reflection coordinates in the laboratory system, can be calculated.

The fourth coordinate system is the projection of the laboratory coordinate system on to the film plane. In order to convert from the laboratory to the film coordinate system we only need to know the crystal to film distance. Figure 4.32 shows the relationship between the crystal, laboratory, and film coordinate systems.

Thus we can calculate the film coordinates for a reflection if we know the angle  $\Phi$  at which this reflection crossed the Ewald sphere.

Let us consider the reciprocal lattice point  $P$  which crosses the Ewald sphere at a rotation angle  $\Phi$ . Figure 4.33 shows that  $P$  is on the Ewald sphere when the centre of the sphere has moved from  $A$  to  $A'$  that is from  $(\lambda^{-1}, 0, 0)$  to  $(\lambda^{-1} \cos \Phi, \lambda^{-1} \sin \Phi, 0)$ .

Since  $P$  lies on the Ewald sphere, its coordinates must satisfy the equation of a sphere

$$(x_0 - \lambda^{-1} \cos \Phi)^2 + (y_0 - \lambda^{-1} \sin \Phi)^2 + z_0^2 = \lambda^{-2}$$

and

$$x_0 \cos \Phi + y_0 \sin \Phi = \frac{1}{2} \lambda (x_0^2 + y_0^2 + z_0^2) \tag{4.32}$$

which can be solved to find the value of  $\Phi$ .<sup>[39]</sup>

Once  $\Phi$  for a reflection is known its coordinates in the laboratory system and its position on the film can be calculated in the way that has been outlined.

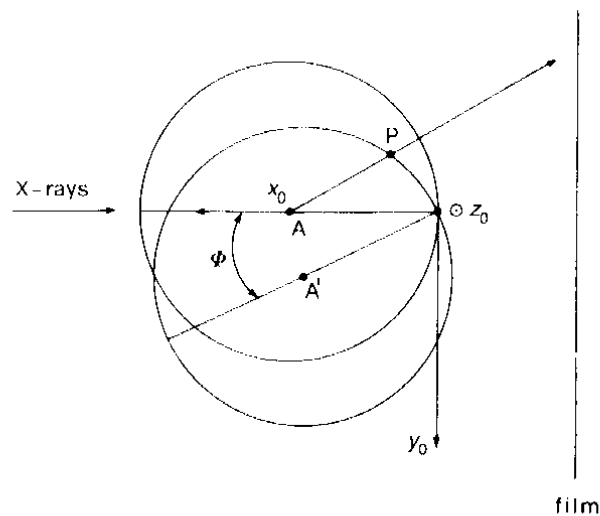


**Fig. 4.33.** When the crystal rotates an angle  $\Phi$  point  $P$  lies on the surface of the Ewald sphere and the centre of the sphere has moved from  $A$  to  $A'$ . The crystal coordinate system is only shown before the rotation, that is when it is coincident with the laboratory system.

## **5.4 X-ray and neutron detectors**

Any particle or kind of electromagnetic radiation can be detected through its interaction with matter. The shape, type, and efficiency of available photon and neutron detectors is directly linked to, and sometimes also determines, the data-collection methods and strategies to be used in the experiment. Film-based cameras were universally used for X-ray experiments until photon counters (i.e. gas-phase proportional detectors and scintillation detectors) with sufficient efficiency were introduced on commercial two- and four-circle diffractometers.<sup>[59]</sup> Then, the search for efficient two-dimensional detectors combining high spatial and time resolution was driven in the last decade by the high photon fluxes available at synchrotron sources. Several one- and two-dimensional PSDs based on different technologies are now commercially available and they are ultimately promoting a diffuse change also in data-collection methods on laboratory instruments. The principal types of X-ray detectors now in use are briefly reviewed: they are based on gas phase-, semiconductor-, and fluorescent-materials. Photographic films and image plates have long been used as two-dimensional detectors, but the formed latent image needs

off-line treatment (film processing and/or film scan) before the data can be electronically stored and analysed. In this context, electronic area detectors are defined as two-dimensional position sensitive devices, which have fast electronic read out and can be re-used for data collection in rapid sequence.

X-ray films are still quite useful but are rapidly becoming obsolete. Image plates are now much in use, especially in macromolecular crystallography, although their technology can probably not be developed much further. The development of the other types of X-ray detectors is a field of active research and substantial advances are expected in the near future.<sup>[23]</sup>

Due to the nature of the neutron absorption by atoms and to the intrinsic weakness of neutron sources, fewer types of efficient neutron detectors are available at this stage, and only minor developments are foreseeable in the near future. Most neutron detectors are gas proportional counters or scintillation detectors. The current effort is to build large arrays of parallel detectors, in order to waste as little scattered signal as possible.

It should be emphasized that no single detection system is currently capable of simultaneous optimal performances in all areas, that is, time resolution, space resolution, and energy resolution. When approaching experimental crystallography, it is therefore, very important to understand the limitations and the advantages of the individual detection system to be selected. The main characteristics that need to be evaluated<sup>[59,60]</sup> are:

1. the **detective quantum efficiency** (DQE), which is a measure of the ability of the detector to absorb incident photons. In the case where Poisson statistics is obeyed, it is defined as  $DQE = N_d/N_i$ , that is the ratio between the number of photons detected by the device  $N_d$  and those incident in the detector window  $N_i$ . The DQE is commonly above 0.5, with values in the range 0.8–0.9 for very efficient detectors,<sup>[61]</sup> and it is typically energy and flux dependent;
2. the **dynamic range** of the detector is the ratio between the maximum and the minimum observable signals. Commonly, the maximum measurable intensity is limited by linearity limits, whereas the minimum intensity is affected by the intrinsic noise of the system. With modern X-ray sources, having highly focused brilliant incident beams, the detector dynamic range required for quality measurement is well in excess of  $10^5$ ;
3. the **detector count rate linearity** refers to the linearity of the DQE with respect to the incident flux.<sup>[62]</sup> In fact, the number of secondary signals per incident photon should remain constant over the full dynamic range of the detector;
4. the **sensitivity** of the detector ( $S$ ) characterizes the minimal quantity of photons per unit time that can be detected relative to the detector background noise. It is commonly defined as  $S = dI/d\varphi$ , where  $dI$  is the current differential corresponding to the increment  $d\varphi$  in the incident radiation flow. The sensitivity strongly depends on the signal-to-noise ratio;
5. the **spectral sensitivity** describes the performance of the detector upon change of the energy of the incident photons. The optimal use of the



- detector over a wide energy range is particularly important at synchrotron sources, where the X-ray source is tunable (Section 5.2.2);
6. the **stability in time** may involve both the detector lifetime (long-term stability) and the stability of the detector over a finite experiment (short-term stability). They both involve the physical or chemical degradation of the detection system and its resistance against radiation damage. The short-term stability is rather important for precise intensity measurement in crystallography. Intensities must be measured within 1 per cent relative errors or better.

A few other properties are especially important for area detectors, such as the **active area**, the **spatial uniformity**, the **spatial resolution**, and particularly for time-resolved diffraction experiments, the **data acquisition rate**. Finally, **energy proportionality** and **energy resolution** may be crucial if the detector is used as a monochromating device or for energy-dispersive diffraction experiments. Table 5.4 summarizes the main detector devices available for X-ray diffraction experiments.

#### 5.4.1 X-ray detectors

As briefly mentioned above, X-ray detectors are based on different physical processes.<sup>[63,64]</sup> In general, detection of photons having energies in the range 5–25 keV involves the excitation of electrons in the detector material. The excitation takes place by photoelectric absorption or Compton scattering. In any case, all or part of the absorbed X-ray photon energy is transferred to the system and secondary processes are activated. These secondary processes may be (1) the ionization of a gas and the formation of electron-ion couples, (2) the generation of electron-hole pairs in a semiconductor, (3) the emission of visible or ultraviolet photons by fluorescence in an inorganic phosphor, or (4) the formation of a latent image by valence change of specific chemical elements in photographic films and plates. In all cases, apart from the specific case of X-ray films, after the initial stage of photon energy conversion, the secondary signal must be converted into electrical energy, amplified, and appropriately stored in digital form. Each detector system therefore, is invariably associated with some kind of readout electronics and data-storage devices.

The dimensionality of the detector system determines the mode of operation during the experiment. **Point detectors** (or zero-dimensional

**Table 5.4** Summary of commonly available X-ray detector systems

System dimensionality	Process of photon detection			
	Gas ionization	Semiconductor	Fluorescence	Chemical process
0-D (point det.)	Proportional photon counters	Solid state detectors. Si(Li), Ge(Li)	Scintillator crystals. NaI(Tl)	
1-D (linear det.)	Linear PSD	Photo-diode arrays		
2-D (area det.)	Multiwire detectors	Charge-couple devices coupled	Phosphors, television area detectors, image plates	X-ray films

detectors, or photon counters) are devices measuring the number of photons impinging on a selected area and returning an electrical signal proportional to the incident photon flux. They have no sensitivity to record the position of the incident photon, and therefore, the spatial information, most often the scattering angle, is determined externally by mechanically positioning the counter at pre-set points with respect to the crystallographic reference system with the use of computer-controlled goniometers. These counters are universally used on single crystal four-circle diffractometers and on polycrystalline specimens two-circle parafocusing goniometers (see further in this chapter for instrument details). **Linear detectors** (or one-dimensional detectors, or linear position sensitive detectors) can measure the number of photons per unit time, but they also record the spatial information of the event with the sensitive elements of the device. When stationary, as is often the case in powder diffraction, they only record a portion of the reciprocal space, and they also need to be moved to scan the whole scattering space. Finally, modern **area detectors** (or two-dimensional detectors, or PSDs) measure the number of photons arriving per unit time as a function of the position within the detector's surface. Such devices, can therefore simultaneously scan a large portion of the reciprocal space, exactly like photographic films, and in addition, they produce digital results in a form suitable for online computer processing and analysis.

#### 5.4.1.1 Point detectors

There are essentially two widely-used kinds of point photon counters:<sup>[59,60]</sup> the proportional gas chambers and the scintillation crystals.

The proportional counters are gas-filled chambers,<sup>[65]</sup> which can be sealed or maintained under constant gas pressure or flow. Used gases are a mixture of noble gases with high  $Z$  (argon, xenon) containing up to 30 per cent polyatomic quenching gas (carbon dioxide, ethane, methane). The noble gas provides the high-absorption material needed for the efficient detection of the incident photons. The quenching gas is added to absorb excess charge and low-energy photons to inhibit unwanted multiple ionization events. When an X-ray photon is absorbed by a noble gas molecule, an inner shell electron is emitted with a kinetic energy, that is, most of the energy of the absorbed photon which is sufficient to produce the ionization of many more molecules. It has been calculated that an X-ray photon of the copper  $K_{\alpha}$  wavelength has enough energy to induce on the average the formation of 320 ion pairs. A high voltage is applied between the outer chamber wall and a central wire, so that ion-electron couples formed by the ionizing photons are accelerated and induce a cascade ionization process known as the Townsend avalanche<sup>[63]</sup> with the formation of several orders of magnitude of new ion pairs. These ion pairs move again in opposite directions under the influence of the electric field and, in so doing, generate the electrical signal that is measured in the detector. The applied voltage is the physical quantity characterizing proportional counters from ionization chambers and Geiger counters. The detection of each incident photon is possible only because of the gas amplification process, which, in the proportionality region is linear. The amplification factor is a function of the

type of gas, gas pressure, electric-field strength, and geometrical configuration. This detection process can be effectively used for photon counting, since each photon triggers an ionization avalanche.

The solid-state scintillation counter is a doped phosphor crystal (or scintillator), commonly NaI(Tl), in which X-ray photons are absorbed and visible blue light is re-emitted. The fluorescent light emission is appropriately amplified and converted into an electrical signal by means of a photomultiplier in optical contact with the scintillator crystal. The photomultiplier tube is composed by an antimony/cesium photocathode emitting a burst of electrons at the arrival of the light photons, and by a series of dynodes that amplify the electron signal and ultimately produce the voltage pulse. The resulting electrical signal is proportional to the total incident photon energy, although the energy resolution is rather low. The scintillator detectors have a low intrinsic noise, a good linearity up to  $10^5$  photons/s if dead-time corrections are properly applied, and a high DQE.

Semiconductor devices based on Si(Li) or Ge(Li) crystals are also used as proportional counters.<sup>[59,60]</sup> They offer the advantage of a high DQE and appropriate energy discrimination, and have been used especially in powder diffraction,<sup>[66]</sup> although the need for permanent cryogenic conditions in order to avoid the drift of the Li ions in the crystals and the relatively large dead time have in practice, limited their diffusion on commercial diffractometers.

Both the excitation of fluorescence in the scintillator crystal and the gas ionization in the counter detector are events that can be triggered by the arrival of only one photon. It can be shown experimentally<sup>[67]</sup> that if an X-ray beam is measured several times with a proportional point detector, the different intensity values obtained follow a Poisson distribution. For such a distribution, the estimated standard deviation, is

$$\sigma = N^{1/2},$$

where  $N$  is the number of counts. The fractional standard deviation is thus

$$\sigma_f = N^{1/2}/N = N^{-1/2}.$$

For diffracted intensities measured by film methods it can be shown that the fractional standard deviation is larger by a factor of 1.35. Thus, intensity measurements performed by diffractometers employing photon counters can be said to be intrinsically more precise than those obtained from film methods.

#### 5.4.1.2 Linear detectors

Linear position sensitive detectors (LPSD) operate as arrays of point detectors, acting as photon counters that, in addition, supply the spatial information of the absorption event. As they survey only a section of the reciprocal space, they are mostly used in powder diffraction, where in most cases only the equatorial portion of the Debye rings is recorded (Section 5.6). The advantage of linear detectors over point counters is straightforward: a sizeable part of the powder-diffraction pattern is

recorded simultaneously, offering substantial improvement over step-scan data collection in terms of counting statistics and/or speed of data acquisition.

There are two major types of LPSD commonly available, corresponding to two different processes of photon detection: the gas-filled proportional chambers based on gas ionization, and the photodiode arrays based on semiconductor technology.

Gas LPSD are designed as gas chambers, in which electron collection and pulse-generating electronics are located at both ends of the anode wire. The material composing the anode is poorly conducting, in order to slow down the passage of electrons and to allow measurement of the rise time of the pulse at each end of the wire. This technique is called delay line, and it allows correlation between the measured time and the position along the wire where the process originated.<sup>[65]</sup> Several manufacturers commercialize short straight gas LPSD for powder diffraction covering a limited portion of reciprocal space, generally an angular range up to  $10^\circ$ – $15^\circ$   $2\theta$ , and which are used for fast stationary measurements, or for rapid scanning of a wider angular range.<sup>[68,69]</sup> When mounted on laboratory Bragg–Brentano diffractometers (Section 5.6.3), they do satisfy the parafocusing condition only in the central portion of the detector, and as a consequence the resolution of the measured powder pattern is rather poor, although the excellent counting statistic allows fast data collection. Another type of curved gas LPSD (CPS120 or CPS590 by INEL)<sup>[70]</sup> is available that uses a thin metallic blade as the anode. It covers a wide angular range ( $90^\circ$  or  $120^\circ$   $2\theta$ ) and has a sample–detector distance constant along the detector. It is used as a fixed detector in Debye–Scherrer geometry (Section 5.6.2), and its main advantage is to record the whole powder-diffraction pattern simultaneously, with no need for angular scan. The device requires careful angular calibration of all channels; this can be done by using a standard powder specimen with accurately known Bragg-peak positions, or by moving the detector through the direct beam.<sup>[71]</sup>

Photodiode arrays<sup>[72]</sup> are one-dimensional arrays of diodes (or pixels) manufactured on a single silicon chip. They are usually available as arrays of 512, 1024, or 2048 pixels with pixel-to-pixel separation of  $25\ \mu\text{m}$  and 2.4 mm height. They include self-scanning electronics for sequential read-out. These devices are commonly not available on commercial powder diffractometers, and have been mostly used for particular time-resolved application with synchrotron radiation.<sup>[73]</sup> They will not be discussed in detail here.

#### 5.4.1.3 Area detectors

Due to its high precision, the four-circle diffractometer equipped with a point detector (Section 5.5.3) is the ideal data-collection instrument for single crystals of small organic molecules and inorganic compounds, but it suffers, as discussed later in detail, from the drawback that it collects only one reflection at a time. When data have to be collected from macromolecular crystals that have very large unit cells and that therefore require the recording of many reflections and which in addition have, in general,

a more or less serious radiation decay problem, the diffractometer is an inadequate data-collection device. On the other hand, the rotation method (Section 5.5.2 and Appendix 5.D.1), that is, with the reflections recorded on film and with a choice of the rotation range  $\Delta\Phi$  made in order to minimize the number of films exposed, and the fraction of partially recorded reflections, has an intrinsically lower precision. This is due to two main reasons; the first is that film is a poorer detector than diffractometer counters; the second is that during the film exposure, the signal is recorded by the film only during a fraction of the total exposure time. If the reflecting range of a reflection of the crystal is  $\Delta$  and the rotation range selected  $\Delta\Phi$ , this fraction is  $\Delta/\Delta\Phi$ . Typically  $\Delta$  is no more than a few tenths of a degree whereas  $\Delta\Phi$  can be one degree or more. In other words, in the rotation method, the signal is recorded on the film during a time equal to  $t\Delta/\Delta\Phi$  where  $t$  is the total exposure time, whereas the background is recorded instead during the total time  $t$ .<sup>[74,75]</sup> One could, in principle, improve this situation by simply reducing  $\Delta\Phi$  so that  $\Delta$  is spanned by several rotation photographs, and then measure the integrated intensities only on those films in which the reflection is found. There are many reasons why this is not done when working with film but this is instead, perfectly feasible when the detection is done by the electronic area detectors.<sup>[76]</sup> These were designed to combine the photon counting efficiency of the diffractometer together with the ability to record a large fraction of the reflections which simultaneously cross the Ewald sphere which is the main advantage of the rotation method. Electronic area detectors, together with image plates, are thus probably the best choice for any kind of diffraction data collection. They are, to date, universally used at synchrotron sources, where the allocated beam time for experiments is limited and there is large demand for fast data collection, but they are now increasingly used in laboratory sources. However, it should be pointed out that some of the devices that are currently available commercially have been optimized for the detection of copper radiation and are, in most cases, less efficient in the detection of the higher-energy molybdenum radiation which is very often used in small-molecule work.<sup>[77]</sup>

#### 5.4.1.4 Principles of operation of electronic area detectors

The most common electronic area detectors that are currently used in diffraction work and that include the presently commercially available instruments belong to three groups, again corresponding to different principles of photon detection: multiwire proportional counters (MWPC) based on gas ionization, television area detectors based on phosphors, and CCD detectors based on semiconductors. We will briefly discuss the basics of these three types of detector.

Multiwire proportional counters are two-dimensional developments of the gas filled chambers described earlier. They contain three parallel planar electrodes; an anode sandwiched in between two cathodes. The anode and at least one of the cathodes are arrays of parallel wires that are perpendicular among them.<sup>[59,78,79]</sup> The gas filling the chamber is usually a xenon-carbon dioxide mixture, as in gas photon counters (see also Mokulskaya

*et al.*),<sup>[80]</sup> and the position of the ionizing event is located from the centre of gravity of the group of resulting cathode pulses. The spatial resolution of the detector is determined by the size of the pixel formed by the electrode wires. There are some limitations in the further development of MWPC detectors. The pixel region defined by the wires cannot be decreased much below 0.3 mm, because of local charge buildup, the point spread function limiting the accuracy with which one can locate the ionization event is rather large, mainly because of ion diffusion and multiple ionization events, and the voltage applied between anode and cathode wires cannot be increased above the proportionality region. Developments in progress attempt to solve these problems by substituting the electrode wires with microstrips (as thin as 50  $\mu\text{m}$ ) obtained by photolithography, by improving the readout mode using wire-by-wire techniques, and by applying gaseous electron multiplier (GEM) foils that enhance the spatial resolution of the device. At present, a major limitation of MWPC is that the overall count rate of the chamber is commonly limited to  $\sim 5 \times 10^5$  counts/s because of dead time. For these reasons MWPC, which had a good share of the market of area detectors on laboratory diffractometers in the late 1980s, and fulfilled the basic requirements of macromolecular crystallographers, are now generally considered obsolete for modern single crystal experiments.<sup>[81]</sup> On the other hand, their excellent dynamic range (better than  $10^6$ ) and the possibility of manufacturing large active areas (over  $200 \times 200 \text{ mm}^2$ ) makes them still very attractive as detectors for small-angle scattering experiments. The existing modern MWPC detectors are mostly non-commercial prototypes available at dedicated synchrotron beamlines.<sup>[82,83]</sup>

In television area detectors, the X-ray radiation is converted into visible light by a fluorescent phosphor. These visible photons, after suitable intensification, are detected by the photocathode of a standard high-sensitivity television camera tube that is linked to a computer.<sup>[84,85]</sup> The area detector phosphor, that is, the fluorescent material that transforms X-rays into visible light is either polycrystalline gadolinium oxysulfide or zinc sulfide and it produces between 250 and 500 visible photons per X-ray photon.<sup>[79]</sup> In spite of this gain in photon numbers, the sensitivity of the camera is not enough to measure them and so, an increase in the signal is required to make it detectable. This enhancement is achieved by an image intensifier in which the photons produced by the first phosphor generate a certain number of electrons from a photocathode which are then accelerated and strike a second phosphor that is optically coupled to the camera. The photon gain of these intensifiers is of the order of either 100 or 1000.<sup>[85]</sup> The television camera tube consists of a photoemissive cathode with an intensifier that accelerates the electrons generated by the light producing a charge image that is scanned by an electron beam that is used to measure the signal. Since the photons arriving in 40 ms, which is the period necessary to scan the image, are not enough to give good counting statistics, a certain number of these images have to be added before the statistics become satisfactory. Several types of fluorescent phosphor detectors, mainly differing in the optical coupling and gaining by the image intensifier, have been available on the market since the late 1980s and have been successfully used for

diffraction data collection on macromolecular crystals, even using synchrotron radiation.<sup>[86–88]</sup> Phosphor screens are now mainly used in connection with CCD devices as radiation shields, or to enhance the active area and the dynamic range.<sup>[89]</sup> Technically, imaging plates are also phosphors, although they are treated separately, because they cannot be operated with direct online readout.

The most recent development in the field of area detectors is the two-dimensional version of semiconductor detectors, which is based on CCD technology.<sup>[59]</sup> CCDs are arrays of independent detector elements (usually  $1024 \times 1024$ , up to  $4096 \times 4096$ ), each composed of a metal-oxide semiconductor (MOS) structure. The single MOS capacitor measures about  $15\text{--}20\ \mu\text{m}$  on the side, and it is suitably biased to establish charge storage volumes. During the serial readout, the charge is transferred from one element to the next until it reaches the output, and the charge packets are moved using two linear, orthogonal registers.<sup>[90]</sup> The transfer circuits are integrated with the elements of the CCD and may be subject to radiation damage. The energy of electron-hole pair formation is very low, so that CCDs have a high dark current (that is, the thermally generated charge) at room temperature and they can work properly as detectors only at liquid-nitrogen temperature. The major advantages are a high efficiency up to high photon energy ( $\sim 20\ \text{keV}$ ), an excellent DQE (close to 0.9), and a potentially high spatial resolution, which depends on the pixel size and the crystal–detector distance. The CCD detectors seem to be suitable for fast data collection both for powder sample and for single crystals. The present limitation is that it is difficult and very expensive to produce CCD arrays with active areas larger than  $\sim 60 \times 60\ \text{mm}^2$ , with most commercial devices having active areas of  $\sim 30 \times 30\ \text{mm}^2$ . The detector needs therefore to be positioned rather close to the sample in order to record a sufficient number of reflections. Depending on the wavelength employed, at present some compromise may be required between the desired angular resolution and the recorder angular range (see Section 5.5.3 for details). CCDs are becoming very popular as substitutes of single counter four-circle diffractometers on laboratory instruments. It has been shown that if diffraction data are collected with sufficient statistics, then the quality of the extracted integrated intensities is comparable to that obtained with conventional four-circle data collection methods.<sup>[91]</sup>

The three types of electronic area detectors described above, together with the image plates described below, have become in the last several years routine devices for crystallographic instrumentation. Most of them are commercially available, and although it is hazardous to compare the relative performances of instrumentation based on diverse technologies, some comparison has been attempted for specific applications.<sup>[76,92]</sup> The present trend is that image plate- and CCD-based diffractometers are increasingly replacing instruments using multiwire proportional counters, television detectors, and conventional photon counters in most laboratories active in single crystal diffraction. Linear gas position sensitive detectors and image plates are increasingly being used in powder diffraction for special applications (such as time-resolved studies, texture

analysis, and high temperature diffraction), although by far most powder diffractometers are still based on proportional counters. Several new types of area detectors are now under development for specific synchrotron-based time-resolved experiments, such as the pixel detectors, the amorphous silicon imagers, and the streak cameras. Although in some cases, they have been used to perform successful experiments with time resolution down to 200 fms, these devices are commonly available only as prototypes and mostly in the research stage.

#### 5.4.1.5 Film as an X-ray detector

The photographic film is effectively a two-dimensional PSD that has been used since the discovery of the diffraction of X-rays by crystals. It offers a number of advantages, namely, the survey of a large portion of reciprocal space, an excellent spatial resolution, the possibility of being flexibly bent following the diffraction geometry, a superb uniform response over the whole sensitive area, a dynamic range of  $10^5$  or better, a DQE close to 1. Its major disadvantages are a low sensitivity, which makes the experiments rather time consuming with laboratory sources, the relatively high intrinsic background noise (film fog) that reduces the precision of the intensity measurement, and especially the very slow readout process, which is probably at present the major factor influencing the rapid obsolescence of film methods.

#### 5.4.1.6 Image plates

The image plate is essentially a storage phosphor. This means that the X-rays photons produce on the plate a latent image that is then excited by stimulation with a He-Ne laser producing light at 633 nm. The light thus generated has a wavelength of 390 nm and is irradiated from the plate areas that were previously hit by the X-ray photons. This phenomenon is called photostimulated luminescence.<sup>[93]</sup> The radiation energy of the X-ray photons can be stored by the phosphor for fairly long periods; it has been found that the photostimulated luminescence is reduced to one-half of its initial value after approximately 10 h. The photostimulable material covering the plate is BaFBr : Eu<sup>+2</sup> crystals. When the plate is hit by X-ray photons some of the Eu<sup>+2</sup> ions are ionized to Eu<sup>+3</sup> ions and the excited electrons are trapped in Br vacancies introduced in the crystal that are called F centres. Subsequent excitation of these centres by the laser liberates again these electrons that return to the Eu<sup>+3</sup> ions which thus become excited Eu<sup>+2</sup> ions. An electronic transition in these ions generates the luminescence with an intensity proportional to that of the original X-rays.<sup>[94]</sup>

The storage phosphor is read by an image reader which releases the stored information by means of the laser and collects the emitted radiation and channels it into a photomultiplier tube that converts the radiation into an electrical signal. The signal is analysed by an image processor producing a pixel digital image. The basic concepts of resolution and optical linearity for image plates are similar to those described above for film, although modern image plates are guaranteed to have a dynamic range of at least  $10^5$ . The plate can be used repeatedly since exposure to visible radiation restores



it to its initial condition. The characteristics of the image reader turn out to be crucial for the performance of the entire system, and the quality and spatial resolution of the image is critically dependent on the reader optics and performance.<sup>[95]</sup> Modern readers can produce images with pixels down to 50  $\mu\text{m}$  in size.

As in X-ray films, the major disadvantage of the image plate is that it cannot generally be read online, although a prototype fast scanner has been developed, which may scan the whole plate in a few seconds.<sup>[96]</sup> Image plates coupled with fast online scanners may effectively be used as area detectors for most static measurements. As far as the dynamic range, spatial resolution, and low background noise are concerned, the image plate to date is among the two-dimensional detectors offering the best overall performance. They are the most-used detectors for macromolecular crystal data collection at synchrotron sources, and they also have proven to yield high-quality powder diffraction data,<sup>[97]</sup> even with samples confined in environmental cells, for example, at high pressure. Translating image plate cameras have also been designed, based on the concept of the old Guinier Lenné cameras (Section 5.6.2), in order to obtain high-quality time-resolved powder diffraction data at synchrotron sources.<sup>[98]</sup> Such experimental setups allow structural and kinetic data to be collected with times comparable with those of solid-state reactions.